Russian Journal of Earth Sciences

Reservoir Characterization and Rock Typing Assessment Utilizing Hydraulic Flow Unit (HFU) and Global Hydraulic Elements (GHE) of Sanga-Sanga Early-Middle Miocene Sandstone, Kutai Basin, Indonesia

E. Komara[*,1], N. Ariyanti[1,2], W. Lestari[1], A. A. Sulaksono[3], N. A. Siddiqui[4], and S. Navisa[1]

[1]Geophysical Engineering, Institut Teknologi Sepuluh Nopember, Surabaya, Indonesia
[2]Geological Engineering, Universitas Gadjah Mada, Yogyakarta, Indonesia
[3]Geology & Geophysics Reservoir Engineer, PT Pertamina Hulu Indonesia Zona 9, Indonesia
[4]Department of Geoscience, Universiti Teknologi Petronas, Perak, Malaysia
* **Correspondence to:** Eki Komara, komara@its.ac.id

Abstract: The heterogeneity characteristics of sandstone reservoirs lead to variations in composition, thickness, and porosity, making them more complex and uneven. This complexity presents a significant challenge in the development of sandstone reservoirs, which is further compounded by contamination factors. To characterize reservoirs comprehensively, the Hydraulic Flow Unit (HFU) method is commonly used. This method can describe reservoir characteristics and determine rock typing distribution based on HFU calculations. In this study, the HFU method is combined with petrophysical parameters and the calculation of oil reserves in the reservoir with the code "MZG." The HFU calculations revealed four rock types, namely RT-1, RT-2, RT-3, and RT-4, in order of decreasing quality from RT-1 to RT-4. Furthermore, this HFU method is integrated with the Multi-Resolution Graph-Based Clustering (MRGC) approach, which serves to spread the available data to wells with limited data, thereby obtaining results that correlate well based on the combination of HFU-derived rock typing and petrophysical parameters. Overall, RT-1 and RT-2 show very good reservoir quality, while RT-3 and RT-4 represent reservoirs with poor quality. This classification has been validated using both qualitative and quantitative approaches based on petrophysical parameters. The correlation between predicted permeability using the GFU (Generalized Flow Unit) method and core data permeability was performed, yielding correlation coefficients of 0.9482 and 0.458, respectively. Oil reserve calculations were carried out based on the geological structure obtained from the structure map derived from seismic picking. The structure reveals an anticline, which was further analyzed considering the impact of petrophysical parameters. Petrophysical calculations using a trial-and-error approach on tortuosity factor (a), cementation exponent (m), and water saturation exponent (n) based on SCAL and RCAL data showed significant results. With parameters a, m, and n set to 1, 2, and 2, respectively, there was an increase in reserves of 31% in tank 1 and 43% in tank 2. This increase was achieved by optimizing higher parameter values based on the SCAL and RCAL data available.

Keywords: Hydraulic flow unit, Rock type, Reservoir Characterization, Petrophysics Parameters, Volumetric Calculation.

Citation: Komara E., Ariyanti N., Lestari W., Sulaksono A. A., Siddiqui N. A., and Navisa S. (2025), Reservoir Characterization and Rock Typing Assessment Utilizing Hydraulic Flow Unit (HFU) and Global Hydraulic Elements (GHE) of Sanga-Sanga Early-Middle Miocene Sandstone, Kutai Basin, Indonesia, *Russian Journal of Earth Sciences*, 25, ES6021, EDN: TNNWYG, https://doi.org/10.2205/2025es001007

Research Article

Received: January 23, 2025
Accepted: June 23, 2025
Published: December 30, 2025

Introduction

The development of sandstone reservoir obstacles in the form of unpredictability and contamination. Global Hydraulic Elements (GHE) are a priori systematic series of Flow Zone Indicator (FZI) values that can be used to define petrophysical elements such as porosity, density, and permeability [*Opuwari et al.*, 2020]. The GHEs are determined based on the FZI values, which are calculated from the permeability and porosity data

[*Amaefule et al.*, 1993]. The reservoir was divided into a number of hydraulic units (HUs) by the GHEs. In order to navigate through permeability and porosity data for reservoir comparison and permeability prediction, the HUs created a basemap [*Corbett and Potter*, 2004]. The use of GHEs and HUs allows for a more accurate and detailed analysis of the reservoir, which can lead to better decision-making in reservoir management. The HFUs approach involves dividing the reservoir into a priori systematic series of FZI values in reservoir characterization [*Guo et al.*, 2007]. The HFUs approach involves dividing the reservoir into a priori systematic series of FZI values, known as GHEs, which are used to define petrophysical elements, known as petrotyping, and create the HFU.

1. Materials and methods

1.1. Geological Setting

The formation of the Kutai Basin can be attributed to extensional processes that occurred in the Middle Eocene, which were then followed by a period of elevation of the basin floor that culminated in the Late Oligocene [*Cloke et al.*, 1999] Figure 1. The elevation of the basin floor in the Kutai Basin was caused by heightened pressure resulting from plate collisions [*Hall and Nichols*, 2002]. This upward movement towards the northwest led to the formation of significant regressive cycles of clastic sedimentation. The state of uplift has experienced minimal disturbance from the Late Oligocene epoch to the present era. This rifting resulted in the formation of a sequence of fault systems that exhibited eastward-dipping extensional characteristics. These fault systems created half-grabens, which subsequently were filled with sediment originating from terrestrial sources and deposited into the adjacent sea. At the conclusion of the Oligocene, evidence indicates widespread contractional deformation and elevation in the western section of the Kutai Basin. During the Early to Middle Miocene, significant tectonic adjustments occurred owing to the rotation of Kalimantan 20–10 Ma, leading to the deformation and uplift of Kalimantan and the inflow of volcanogenic clastics into the Kutai Basin from western terranes. The confluence of the microcontinental block with the subduction zone at the northwest edge of Kalimantan (Palawan Trench) resulted in elevation, forming the Central Kalimantan Mountains. In the Sangasanga region, this corresponds to a shelf consisting of Miocene sandstones and carbonates, which is overlain by an outer shelf, subsequently covered by sandstones and shales from the progradational system of the Miocene Mahakam Delta [*McClay et al.*, 2000].

The beginning of the Middle Miocene (~14.0 Ma) marks the onset of a major period of basin inversion in Sangasanga [*McClay et al.*, 2000]. Progressive deformation migrated from west to east, with east-dominant reverse faults and the migration of depocenters within the Kutai Basin. The collision of the Banggai-Sula area in Sulawesi during the Late Middle Miocene (10.5 Ma) led to increased depocenter shifting and inversion in the eastern section of the Kutai Basin. In the Early Pliocene (6.5 Ma), structural inversion and progressive eastward shifting of depocenters continued. During the Pliocene-Pleistocene, inversion and uplift of the Southern Meratus Mountains from the Kutai Basin indicate ongoing contraction. The Mahakam Fold Belt had a phase of late tightening and thrusting, which predominantly took place inside the anticlines located in the Sangasanga Block. The primary tectonic compressional phase is understood to be the consequence of the collision between the Indo-Australian plate and the Banda Arc [*Satyana*, 2006]. Throughout the history of Kutai Basin inversion from the Middle Miocene to the present, a dominant northwest-directed trend is deduced from relative plate movements and the major fold structure trends. This trend is observable both onshore and offshore and has been confirmed through drilling studies in the Kutai Basin.

The petroleum systems of the Kutai Basin are characterized by hydrocarbon source rocks consisting of shale and coal deposits dating from the Early Miocene to Middle Miocene, primarily found within the Pamaluan, Pulubalang, and Balikpapan Formations [*Chambers and Daley*, 1997]. The lithological types serving as reservoir rocks within the Sangasanga Block are sandstone facies formed as a result of regressive sedimentation

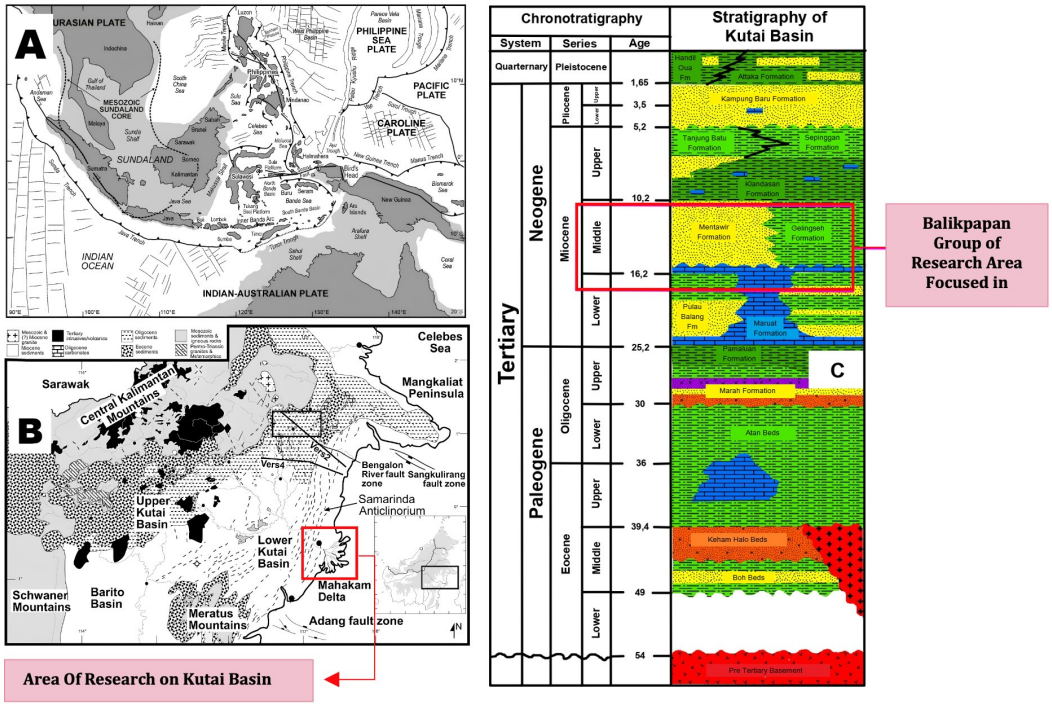

Figure 1. Regional Geology of Indonesia (a), Regional Geology of Kalimantan (The area marked with a box indicates the research area located in the Kutai Basin) (b), and The stratigraphic chart highlights the research interval with pink boxes, representing the Early to Middle Miocene sandstone facies of the Balikpapan and Kampung Baru Formations, with the color legend as follows: Green for shale, Yellow for sandstone, Blue for carbonate rock, Purple for siltstone, Orange for conglomerate rock, and Red for the pre-tertiary basement (c).

within the deltaic system. These specific sandstone facies, known as the Balikpapan and Kampung Baru Formations, have been accurately dated through biostratigraphic analysis to encompass an age range spanning from the Middle Miocene to the Late Miocene/Early Pliocene.

1.2. Reservoir Geology

Referring to various existing studies, these balikpapan group reservoir sandstone facies typically exhibit good to excellent porosity, with porosity values ranging from 15% to 30% [*Musu et al.*, 2017]. The impermeable rocks acting as cap rocks in the Sangasanga Block are relatively thick shale beds, generally deposited in environments within Late Miocene deltaic system, which are younger than the sandstone layers acting as reservoir rocks. The hydrocarbon trapping systems in the Kutai Basin are dominated by structural traps formed by anticlines and upthrust and normal or inversion faults, as well as combinations of these structural elements [*Cloke et al.*, 1999]. Hydrocarbon migration is believed to occur through two main mechanisms. First, vertical migration from older source rocks stratigraphically located deeper, such as the upper portions of the Pulubalang Formation, which can migrate through fault pathways. Second, lateral migration, primarily originating from organic-rich shale layers of the same age as the reservoir rocks, sourced from the Balikpapan Formation itself.

1.3. Hydraulic Flow Unit

A Hydraulic Flow Unit (HFU) is characterized as a volume of rock in which the constituents have relatively uniform fluid flow characteristics, distinct from those in other units [*Ebanks*, 1987]. The concept of HFU differs from lithofacies as it aims to group similar fluid pathways within a reservoir rather than being based on lithological distribution [*Abdulelah et al.*, 2018]. HFUs can be determined by utilizing the reservoir quality index,

pore matrix ratio, and flow zone indicator [*Adrianto*, 2018]. After the HFU parameters calculation, the results of HFUs parameters used to reservoir rock type determination.

$$\begin{aligned}
\sqrt{\frac{K}{\phi_e}} &= \left(\frac{1}{F\tau^2 S_{gv}^2}\right)\left(\frac{\phi_e}{(1-\phi_e)}\right) \\
RQI &= 0.0314\sqrt{\frac{k}{\phi}} \\
\phi_z &= \frac{\phi}{1-\phi} \\
FZI &= \frac{RQI}{\phi_z} \\
k &= 1014(FZI)^2\left(\frac{\phi_e^3}{(1-\phi_e)^2}\right)
\end{aligned} \tag{1}$$

1.4. Discrete Rock Type

Amaefule et al. [1993] propose the discrete rock type (DRT) methodology, which entails classifying reservoirs into various rock type reservoirs (RRTs) according to the FZI parameter. This method involves categorizing the reservoir into several rock kinds with the formula shown below [*El-Sawy et al.*, 2020].

$$\text{HFU or DRT} = \text{round}(2\ln(FZI) + 10.6)),$$

where, DRT is the discrete rock type and FZI is the flow zone indicator in μm.

1.5. Global Hydraulic Elements

Global hydraulic elements refer to a predetermined and organized set of Flow Zone Indicator (FZI) values that serve the purpose of delineating petrophysical features, commonly referred to as petrotyping. The Global Hydraulic Elements were determined based on the FZI values, which are calculated from the permeability and porosity data of the reservoir. The Global Hydraulic Elements serve to partition the reservoir into many hydraulic units (HFUs). The HFUs were used to develop a basemap and atlas for traversing permeability and porosity data for reservoir comparison and permeability forecasting. Consequently, the Global Hydraulic Elements are established according to the FZI values, derived from the reservoir's permeability and porosity data. *Corbett and Potter* [2004] used the term 'petrotype' to define a specific category of petrophysical rock types, denoting a collection of global hydraulic elements (GHE) distinguished by a systematic configuration of FZI values and designated graphs in accordance with the Kozeny–Carman equation,

$$K = \phi\left(\text{FZI}\cdot\frac{\phi/(1-\phi)}{0.0314}\right)^2.$$

The GHE technique utilizes an ordered arrangement of FZI values to effectively cluster data and discern distinct fields that have similar petrophysical features and geological significance. Trends can be easily determined by plotting plug data on the GHE's 'basemap' and these trends can convey geologic meaning shown on Figure 2. To distinguish between various rock types, one can also achieve this differentiation by grouping them based on their corresponding FZI values cutoff of each GHE rock type, as exemplified in Table 1.

1.6. Multi Resolution Graphed Based Clustering

The MRGC framework is a comprehensive methodology that utilizes a combination of geostatistical and neural network techniques to analyze changes in log behavioral responses through a multi-dimensional dot pattern idea. This method relies on parameters such as *k*-nearest neighbors and data graphs, as shown in Figure 3 . The objective of the clustering process is to categorize data points that exhibit similarities into a single cluster, while

Table 1. FZI cutoff values for each GHE rock type used to group rock types

FZI	GHE	FZI	GHE
48	10	1.5	5
24	9	0.75	4
12	8	0.375	3
6	7	0.1875	2
3	6	0.0938	1

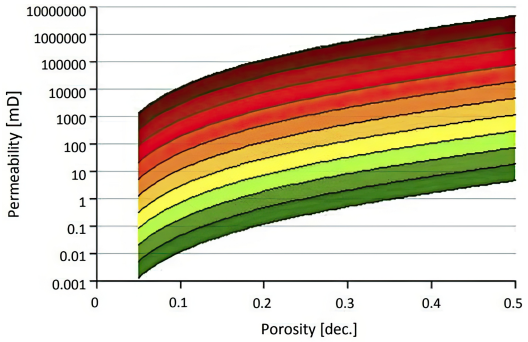

Figure 2. Global Hydraulic Elements Basemap.

ensuring that dissimilar data points are allocated to separate clusters. In the Minimum Redundancy Maximum Gain Clustering (MRGC) algorithm, the process of partitioning the data into clusters is performed in an automated manner, with the objective of optimizing the clustering based on the density, size, and shape characteristics of the input data. Within the context of MRGC (Multi-Resolution Graph Clustering), the aforementioned clustered points, referred to as dot clusters, are organized into distinct groups known as electrofacies. These electrofacies are subsequently linked to variations in rock attributes and validated by the comparison with rock type findings derived from core data [*Ye and Rabiller*, 2000].

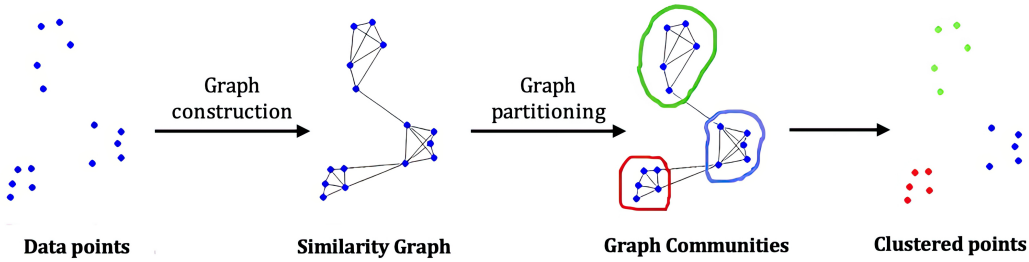

Figure 3. *K*-Nearest Neighbors Algorithm works in MRGC Method.

2. Result and Discussion

2.1. Core Data HFU

Before processing the core data, it is important to note that based on the SCAL and RCA data readings, the core data falls into the 'water' category. This data range spans from 890.60 m to 905.65 m. According to the core data, within the studied Balikpapan Formation, three lithological categories were identified: a) depth 890.60 m to 898.19 m, with combination of sandstone and claystone; b) depth 898.19 m to 898.74 m, with claystone and thin silt interbeds; and c) depth 898.74 m to 906.65 m. with sandstone. In the core data processing based on porosity and permeability data, calculations of hydraulic flow unit parameters were performed using the method presented in (1). Results of the hydraulic flow unit parameter processing shows what explain these results as these are main results on Table 2.

Table 2. Hydraulic flow unit parameter results

Depth	Total Porosity (%)	Porosity (Dec)	Permeability	Reservoir Quality Index	Normalized Porosity (PHIZ)	Flow Zone Indicator	Discrete Rock Type	Perm Prediction (md)
891.8	23.7	0.237	563	1.530417	0.310616	4.927037	5.5	1299.019
891.85	22.8	0.228	337	1.207195	0.295337	4.085175	5.37	1068.7
900.8	22.5	0.225	173	0.870686	0.290322	2.990083	5.22	194.876
894.5	21.8	0.218	98.1	0.666095	0.278772	2.389835	5.13	167.048
898	22.3	0.223	94.3	0.645703	0.287072	2.248925	5.11	186.514
900.3	20.6	0.206	66.4	0.563742	0.259446	2.178681	5.09	127.721
902.8	21.6	0.216	66.7	0.55118	0.27551	2.002755	5.07	159.8037
905.5	22.8	0.228	78.6	0.583007	0.293537	1.97404	5.06	208.0787
893.8	18.8	0.188	32.1	0.410306	0.231521	1.772153	5.03	84.29205
891.3	18.1	0.181	26.9	0.382795	0.221001	1.732095	5.02	71.34257
897.3	21.4	0.214	42.1	0.440417	0.272265	1.61766	5.01	152.8498
902.7	18.8	0.188	17.7	0.304675	0.231527	1.315958	4.96	23.69262
894.77	19.9	0.199	20.3	0.317140	0.248439	1.27652	4.95	30.60543
894.9	20	0.2	16.6	0.286067	0.25	1.144270	4.93	31.31571
902.4	18.9	0.189	14.2	0.272171	0.233046	1.167901	4.93	24.25764
899.8	20.6	0.206	16.6	0.281871	0.259446	1.086434	4.92	35.89973
904.7	22.2	0.222	23.5	0.323063	0.285347	1.132175	4.92	51.28549
903.8	21.1	0.211	17.1	0.282674	0.267421	1.057042	4.91	40.17718
896.5	18.8	0.188	9.71	0.225662	0.231521	0.974672	4.9	23.69262
893	16	0.16	4.67	0.169639	0.190476	0.890687	4.88	11.88851
893.78	17.4	0.174	4.79	0.164748	0.210653	0.782084	4.86	16.91365
896.1	17.9	0.179	5.13	0.168097	0.218063	0.770996	4.86	19.1078
903.3	14.1	0.141	0.934	0.080158	0.164144	0.492342	4.81	1.110348
899	15.3	0.153	0.974	0.079225	0.180643	0.438586	4.8	1.539983
890.8	17	0.17	1.05	0.078037	0.204819	0.38100	4.79	2.38355
893.5	11.8	0.118	0.265	0.047056	0.133787	0.351721	4.79	0.559082

Upon performing the calculation of the hydraulic flow unit, discrete values for rock types were acquired and are presented on Table 2 and Table 3. The determination of rock types is not exclusively reliant on the discrete rock type equation, since it necessitates supplementary validation to reinforce the accuracy of the assigned rock type values. Following this, a correlation was established between core porosity and core permeability, as well as between Normalized porosity and reservoir quality index on Figure 4a. This procedure was conducted in order to get insight into the distribution patterns of fundamental data values and to segment the data distribution by visually delineating gradient lines across the data dispersion. Furthermore, the verification of rock type identification was conducted by generating scatter plots that compared the outcomes of Mercury Injection Capillary Pressure study with wetting phase saturation. The outcomes obtained from the analysis of these three parameters for the purpose of rock type determination will provide the optimal quantity of rock types.

Subsequently, based on the Discrete Rock Type (DRT) classification with a limit of 4 rock types determined by the scatter plot of the HFU parameter, the following results were obtained, The four identified rock types are categorized, with RT-1 representing the

Table 3. Discrete rock type values

Depth	Discrete Rock Type	Depth	Discrete Rock Type
891.8	5.49	894.9	4.93
891.85	5.37	902.4	4.93
900.8	5.22	899.8	4.92
894.5	5.13	904.7	4.92
898	5.11	903.8	4.91
900.3	5.09	896.5	4.90
902.8	5.07	893	4.88
905.5	5.06	893.78	4.86
893.8	5.03	896.1	4.86
891.3	5.02	903.3	4.81
897.3	5.01	899	4.80
902.7	4.96	890.8	4.79
894.77	4.95	893.5	4.79

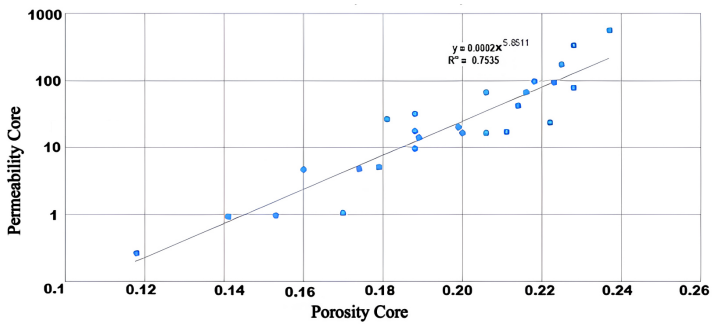

(a)

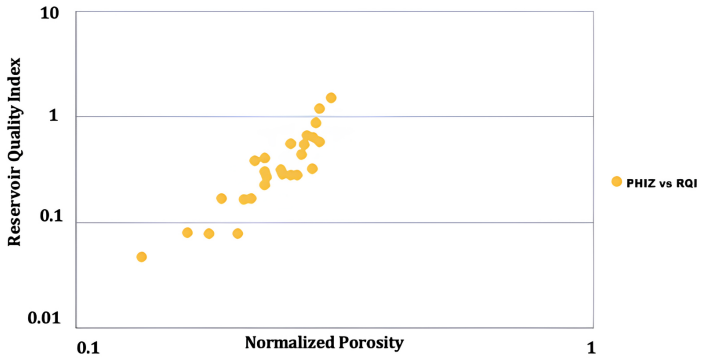

(b)

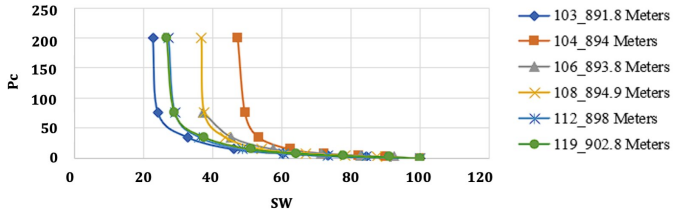

(c)

Figure 4. Rock Typing Determination Parameters (a) Porosity core and permeability core plot, and (b) normalized porosity and reservoir quality index plot, (c) air brine capillar.

most favorable (best) reservoir rock type, and RT-4 denoting the least favorable (poorest) reservoir rock type (presented in the Table 4 and Figure 5).

Table 4. Final results of rock type classification based on HFU method

Depth	Flow Zone Indicator	Rock type	Depth	Flow Zone Indicator	Rock type
891.8	4.927037463	1	894.9	1.144270458	3
891.85	4.087517531	1	902.4	1.167890076	3
900.8	2.999028721	1	899.8	1.086434039	3
894.5	2.389385173	2	904.7	1.132175401	3
898	2.249827488	2	903.8	1.057014691	3
900.3	2.172868078	2	896.5	0.974672064	3
902.8	2.002755813	2	893	0.890609658	3
905.5	1.974040011	2	893.78	0.782084322	3
893.8	1.772153838	2	896.1	0.770995674	3
891.3	1.732095477	2	903.3	0.492342788	4
897.3	1.617605378	2	899	0.438586632	4
902.7	1.315938329	3	890.8	0.381003537	4
894.77	1.276528656	3	893.5	0.351720887	4

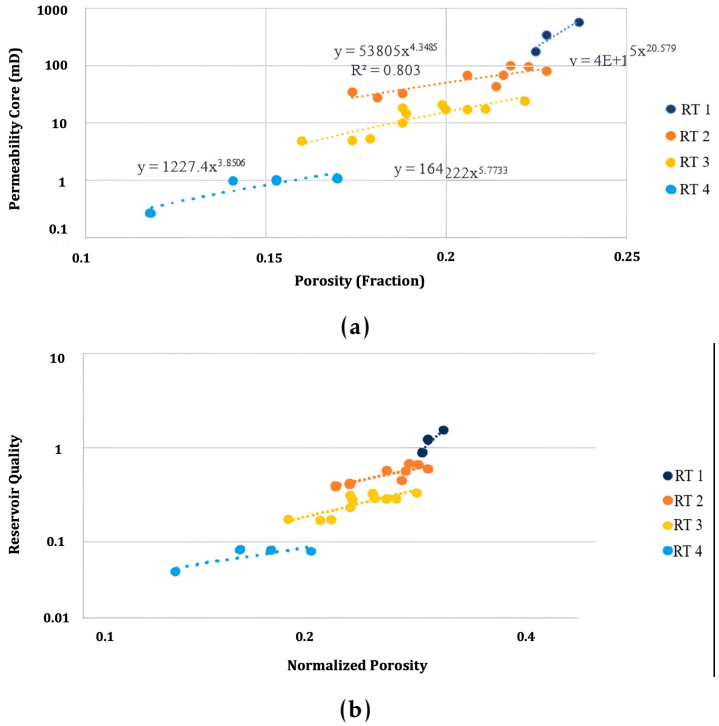

Figure 5. (a) Plotting with Rock typing (a) Porosity Core vs Permeability Core and (b) Normalized Porosity vs Reservoir Quality index.

After completing calculations and rock type determination, to validate the results, permeability prediction based on hydraulic flow unit was calculated using the formula on method. The results of the coefficient correlation value is relatively high it means that the correlation of permeability prediction based on regression trendline is near perfect with 0.8758 shown on Figure 6.

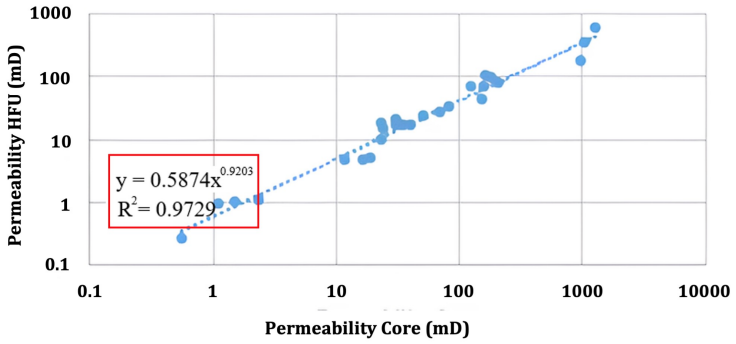

Figure 6. Correlation Between Permeability HFU and Permeability.

2.2. Core Data GHE

The identification of rock types in the global hydraulic elements (GHE) approach is based on the assessment of porosity and permeability, which are then utilized to construct a plot using the GHE formula [*Corbett and Potter*, 2004]. In order to differentiate between different types of rocks, the graph is cross-referenced with the basemap, and the table presents the maximum and lowest values of the Flow Zone Indicator (FZI) for each GHE rock type, as depicted in section 2. It is worth mentioning that, akin to the Hydraulic Flow Unit methodology, the categorization of rock types is conducted into four distinct classifications. The findings derived from both the global hydraulic flow unit and hydraulic flow unit approaches exhibit a high degree of similarity, with only a single core sample displaying variation between the two rock typing methodologies, as illustrated in the table and graphs provided thereafter on Table 5 and Figure 7.

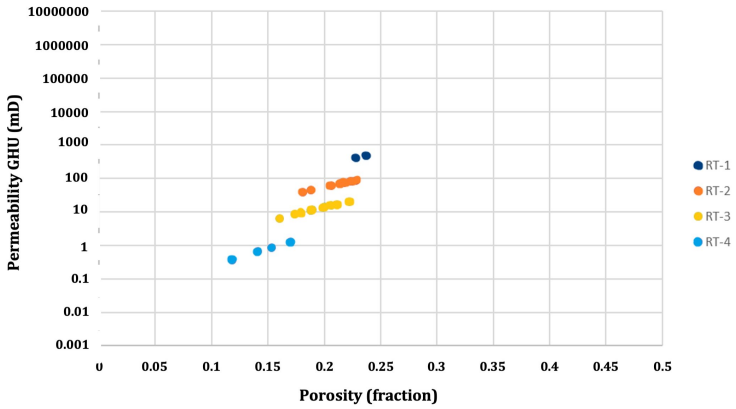

Figure 7. Correlation between permeability GHU prediction with permeability core.

Upon completing the calculations and rock type determination, a validation step was carried out by predicting permeability based on global hydraulic elements using the formula outlined in section 2. The results indicated a high coefficient correlation value, with a value of 0.9418. This high correlation coefficient on Figure 8 suggests that the permeability prediction based on the regression trendline is nearly perfect, indicating that the permeability prediction based on global hydraulic elements outperforms the hydraulic flow unit method in terms of accuracy and reliability.

2.3. Validate Thin Section

After obtaining the rock type classifications, a scatter plot was created to visualize the distribution of the resulting values based on the core data and rock type assignments. The scatter plot revealed that, as shown in the figure, the rock type distribution, when analyzed with the provided regression trendline, yielded fairly good coefficient values. Therefore, the rock type assignments based on the core data appear to be quite relevant.

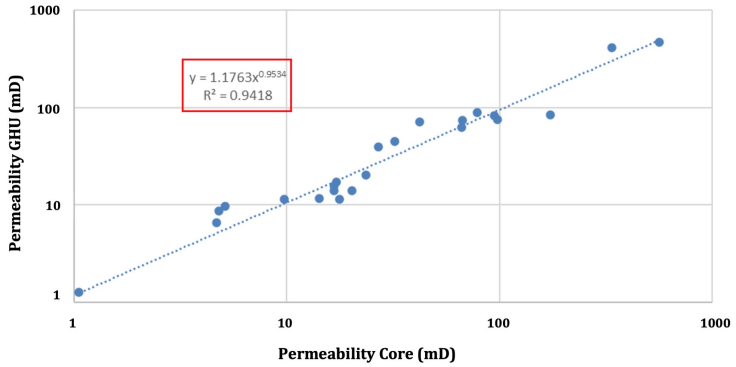

Figure 8. Correlation between permeability GHU prediction with permeability core.

Subsequently, an interpretation was conducted, incorporating correlations between thin section data (petrography) obtained from core reports (SCAL & RCA).

2.4. MRGC

Subsequently, in Figure 9 and Figure 10, the correlation between thin section data and petrography results was obtained, along with the rock type classifications in the scatter plot. Here are the findings for each rock type: (1) RT-1: It was determined to be medium-

Table 5. GHE Parameters Result

Depth	Total Porosity (%)	Porosity (Dec)	Permeability	Reservoir Quality Index	Pore Matrix Ratio (Normalized Porosity)	Flow Zone Indicator	Discrete Rock Type	Rock Type GHE	Rock type Final GHE	FZI Mean GHE	Perm Prediction (md)
891.8	23.7	0.237	563	1.530417	0.310616	4.927037	5.5	7	1	4.5072775	1299.019
891.85	22.8	0.228	337	1.207195	0.295337	4.085175	5.37	7	1		1068.7
900.8	22.5	0.225	173	0.870686	0.290322	2.990083	5.22	6	2		194.876
894.5	21.8	0.218	98.1	0.666095	0.278772	2.389835	5.13	6	2		167.048
898	22.3	0.223	94.3	0.645703	0.287072	2.248925	5.11	6	2		186.514
900.3	20.6	0.206	66.4	0.563742	0.259446	2.178681	5.09	6	2		127.721
902.8	21.6	0.216	66.7	0.55118	0.27551	2.002755	5.07	6	2	2.10108444	159.8037
905.5	22.8	0.228	78.6	0.583007	0.293537	1.97404	5.06	6	2		208.0787
893.8	18.8	0.188	32.1	0.410306	0.231521	1.772153	5.03	6	2		84.29205
891.3	18.1	0.181	26.9	0.382795	0.221001	1.732095	5.02	6	2		71.34257
897.3	21.4	0.214	42.1	0.440417	0.272265	1.61766	5.01	6	2		152.8498
902.7	18.8	0.188	17.7	0.304675	0.231527	1.315958	4.96	5	3		23.69262
894.77	19.9	0.199	20.3	0.317140	0.248439	1.27652	4.95	5	3		30.60543
894.9	20	0.2	16.6	0.286067	0.25	1.144270	4.93	5	3		31.31571
902.4	18.9	0.189	14.2	0.272171	0.233046	1.167901	4.93	5	3		24.25764
899.8	20.6	0.206	16.6	0.281871	0.259446	1.086434	4.92	5	3		35.89973
904.7	22.2	0.222	23.5	0.323063	0.285347	1.132175	4.92	5	3	1.0544194	51.28549
903.8	21.1	0.211	17.1	0.282674	0.267421	1.057042	4.91	5	3		40.17718
896.5	18.8	0.188	9.71	0.225662	0.231521	0.974672	4.9	5	3		23.69262
893	16	0.16	4.67	0.169639	0.190476	0.890687	4.88	5	3		11.88851
893.78	17.4	0.174	4.79	0.164748	0.210653	0.782084	4.86	5	3		16.91365
896.1	17.9	0.179	5.13	0.168097	0.218063	0.770996	4.86	5	3		19.1078
903.3	14.1	0.141	0.934	0.080158	0.164144	0.492342	4.81	4	4		1.110348
899	15.3	0.153	0.974	0.079225	0.180643	0.438586	4.8	4	4	0.41591346	1.539983
890.8	17	0.17	1.05	0.078037	0.204819	0.38100	4.79	4	4		2.38355
893.5	11.8	0.118	0.265	0.047056	0.133787	0.351721	4.79	4	4		0.559082

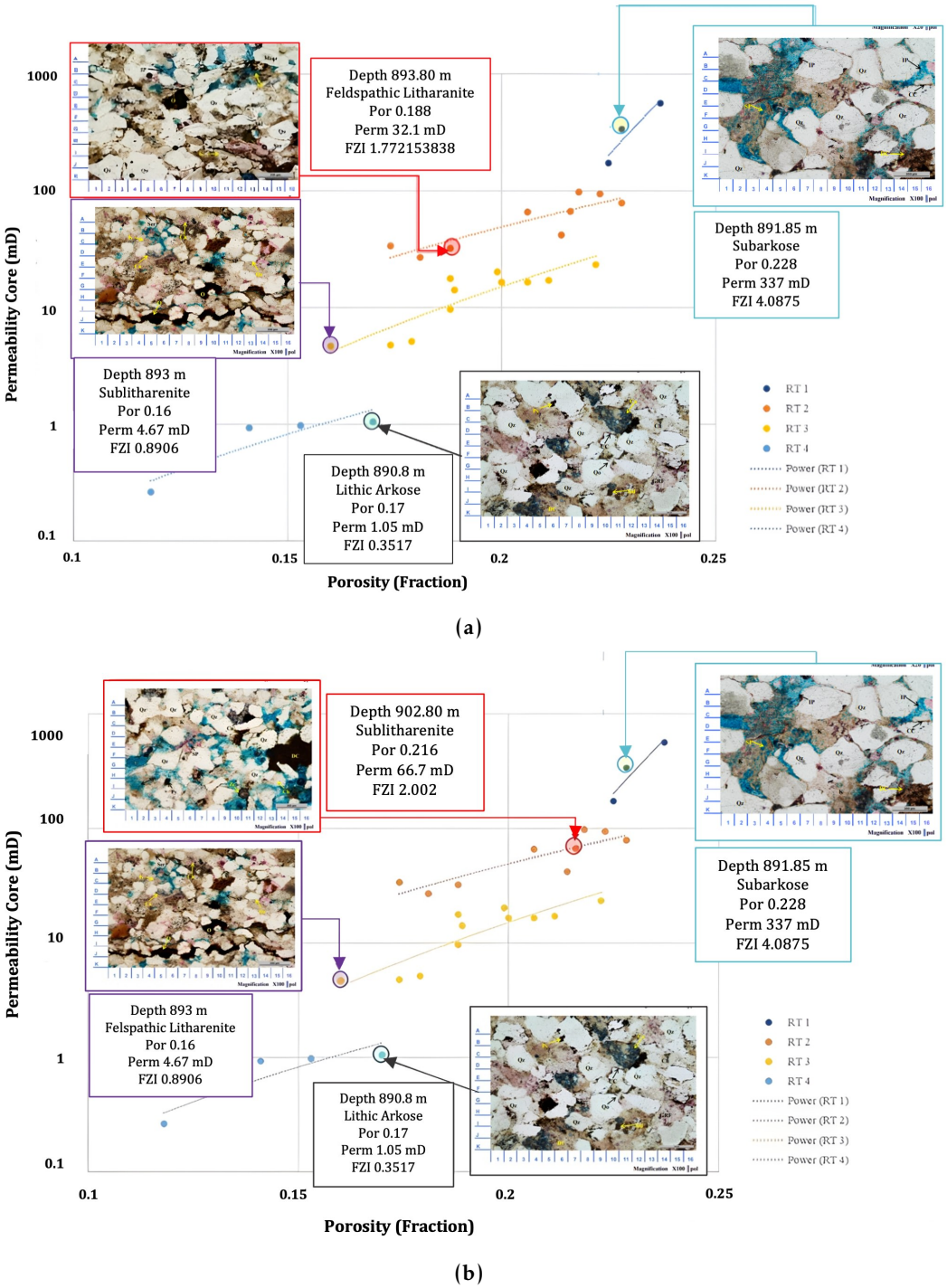

Figure 9. Scatter Plot between Porosity and Permeabilty with Thin Section each Rock Type Method (a) Hydraulic Flow Unit and (b) Global Hydraulic Unit.

grained sandstone, well-sorted, classified as subarkose with subangular to rounded grains, mostly exhibiting contacts followed by planar contacts; (2) RT-2: Identified as fine-grained and well-sorted sandstone, classified as sublitharenite. It is composed mainly of quartz with rock fragments (chert, metaquartzite, granitic type, schist, sandstone, volcanic type, and claystone), plagioclase, K-feldspar, and organic material; (3) RT-3: Found to be very fine-grained and well-sorted sandstone, classified as feldspathic litharenite. It contains quartz with rock fragments (chert, sideritic clast, metaquartzite, schist, granitic and volcanic type, sandstone, calcareous debris), plagioclase, K-feldspar, and other minerals such as muscovite, zircon, and hematite; (4) RT-4: Identified as fine-grained and well-sorted

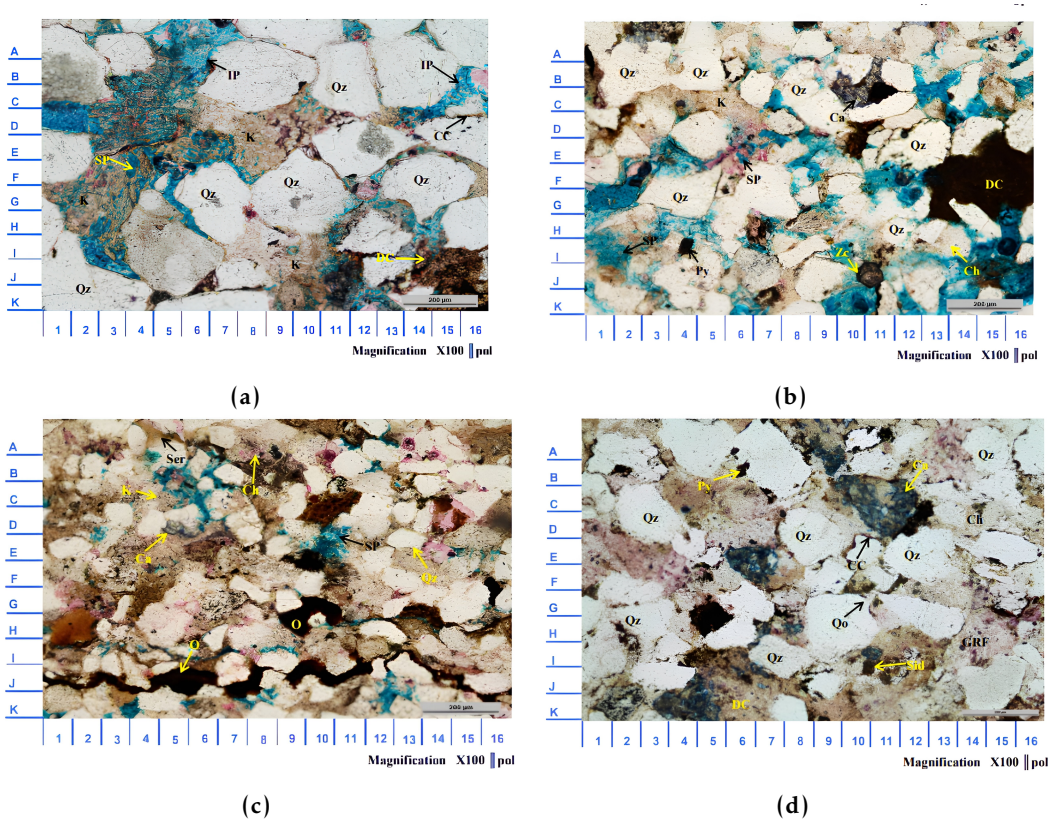

Figure 10. Thin Section of Each Rock Type (a) I – Subarkose sandstone, (b) II – Sublitharenite sandstone, (c) III – Feldspathic Litharenite sandstone, and (d) IV – Lithic Arkose sandstone. (Qz: Quartz, O: Oil, Py: Pyrite, Mtqz: Meta Quartz, Sc: Schist, C: Chert, Zc: Zircon, K: K-feldspar).

sandstone, classified as lithic arkose. It consists of subangular to rounded grains with some points indicating planar contact boundaries. The composition includes quartz, rock fragments (cherty, granitic type, metaquartzite, calcareous debris, and sandstone), plagioclase, K-feldspar, and additional minerals like muscovite, zircon, and organic material. These findings were then combined with the descriptions of other core data that had petrographic information. A summary of the rock types mentioned is presented in the Table 6 and Table 7.

Table 6. Summary of Rock Typing Results of GHU Method

Rock type	Parameter	Value			Lithology	Texture
		Min	Mean	Max		
1	Porosity	0.228	0.2325	0.237	Subarkose	Massive
	Permeability	337	450	563		
	FZI	4.088	4.51	4.92703746		
2	Porosity	0.181	0.211	0.228	Feldsphatic Litharenite Sublitharenite	Bioturbated, Massive, Faintly Laminated
	Permeability	26.9	75.355556	173		
	FZI	1.61760538	2.1	2.99903		
3	Porosity	0.16	0.1923636	0.222	Sublitharenite	Massive Faintly Laminated
	Permeability	4.67	13.663636	23.5		
	FZI	0.77099567	1.0544194	1.31593833		
4	Porosity	0.118	0.1455	0.17	Lithic Arkose	Massive
	Permeability	0.265	0.80575	1.05		
	FZI	0.35172089	0.4159135	0.49234279		

Subsequently, after obtaining the hydraulic flow unit and rock type data, the distribution of rock types in the 'MZG' reservoir marker and the distribution across all other wells was conducted using the Multi-Resolution Graph Based Clustering method. This distribution process was carried out in two stages. The first stage involved the distribution with the marker alone from petrophysics analysis, and the second stage involved spreading the distribution to all wells, both horizontally and vertically.

Based on the distribution of rock types, as depicted in the provided figure, it is evident that the rock type predictions using the Multi-Resolution Graph Based Clustering (MRGC) method, particularly in the MZG-1 well, or any well with core data, closely match the pre-identified rock type data with an accuracy exceeding 75%. The rock type prediction derived from global hydraulic elements (GHE) exhibits a somewhat superior performance in comparison to the rock type prediction derived from hydraulic flow units (HFU), since GHU yields one less distinct prediction than HFU. As we can see on Figure 10 the rock type classification and prediction using GHU is more pessimistic than using HFU, but we know that both of RT-1 and RT-2 is considered good quality reservoir, therefore it is fine despite the differences of the prediction. Indeed, it is observed that the rock type classification and prediction using the Global Hydraulic Elements (GHU) approach may be more pessimistic compared to using the Hydraulic Flow Unit (HFU) method. However, it is important to note that both RT-1 and RT-2 are considered to represent good quality reservoirs.

These differences in prediction between GHU and HFU may arise from variations in the underlying assumptions and parameters used in each method. Despite the disparities in prediction, the fact that both RT-1 and RT-2 are identified as good quality reservoirs is reassuring. The characterization of rock typing based on the presented log parameter data, including Gamma ray, Bulk density, Neutron Porosity, V_{shale}, V_{coal}, Total Porosity, and Effective Porosity, can have variations and may not always result in 100% similarity between rock types. Several factors contribute to this variation: 1) Core Data Variability: The core data obtained may represent various electrofacies, and in some cases, the samples may not have been collected under optimal conditions (e.g., damaged or fragmented samples). 2) Algorithmic Approach: The use of the k-Nearest Neighbors algorithm can result in selecting the best-fit values based on the propagation of log parameters and rock typing. This means that for certain depth intervals, where multiple core-based rock typing data points exist (e.g., within the depth range of 893 m to 894 m), the algorithm selects the best-suited rock typing values, leading to narrower ranges.

In Figure 11b and 11c, specifically in wells MZG-2 and MZG-3, the rock type determination aligns well with the presence of hydrocarbon-bearing oil. However, for MZG-1, the determined rock type suggests the presence of fresh water. In the characterization

Table 7. Summary of Rock Typing Results of HFU Method

Rock type	Parameter	Value			Lithology	Texture
		Min	Mean	Max		
1	Porosity	0.225	0.23	0.237	Subarkose	Massive
	Permeability	173	357.66667	563		
	FZI	2.99902872	4.0045279	4.92703746		
2	Porosity	0.181	0.20925	0.228	Feldsphatic Litharenite Sublitharenite	Bioturbated, Massive, Faintly Laminated
	Permeability	26.9	63.15	98.1		
	FZI	1.61760538	1.9888414	2.38938517		
3	Porosity	0.16	0.1923636	0.222	Sublitharenite	Massive Faintly Laminated
	Permeability	4.67	13.663636	23.5		
	FZI	0.77099567	1.0544194	1.31593833		
4	Porosity	0.118	0.1455	0.17	Lithic Arkose	Massive
	Permeability	0.265	0.80575	1.05		
	FZI	0.35172089	0.4159135	0.49234279		

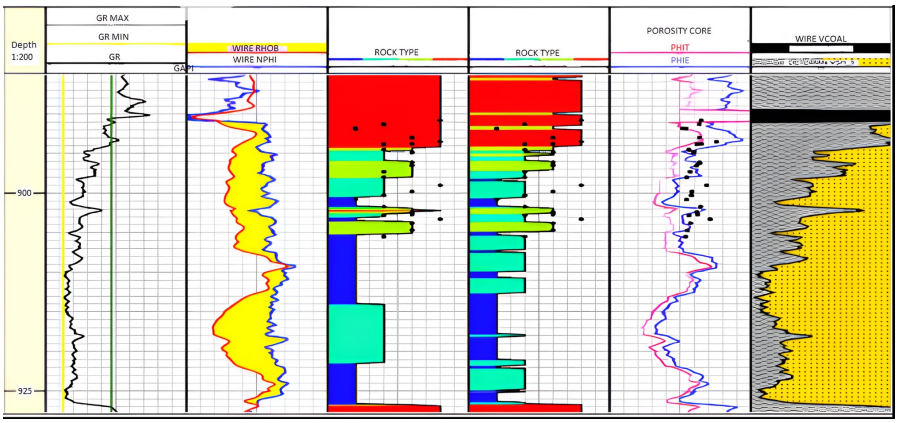

(a)

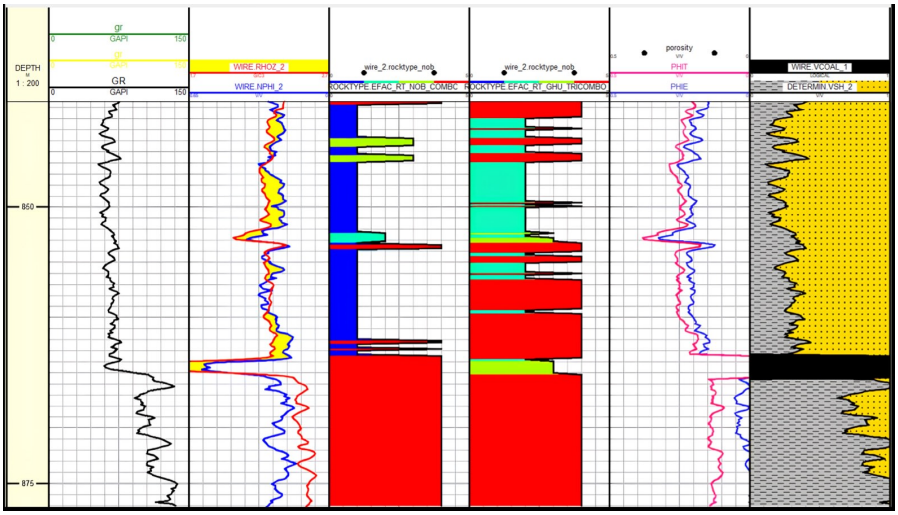

(b)

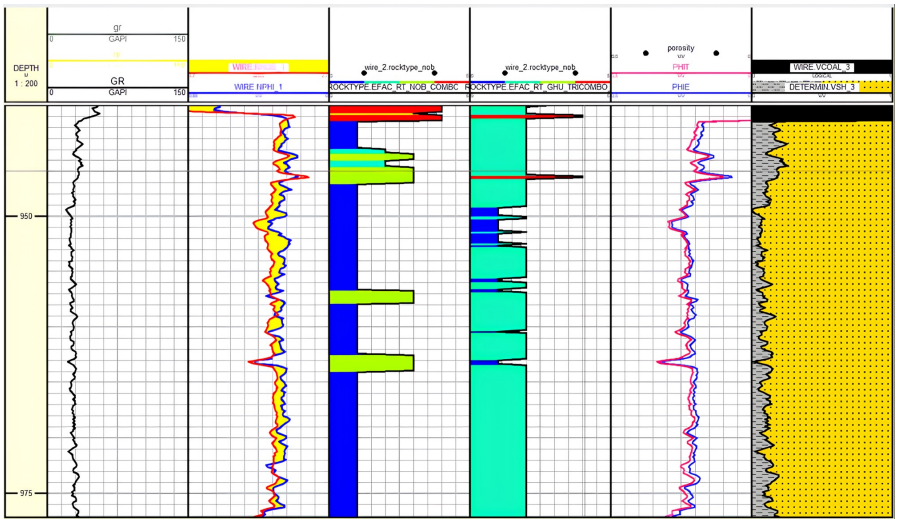

(c)

Figure 11. Results of MRGC Distribution HFU and GFE on (a) X-1 Well, (b) X-2 Well, and (c) X-3 Well.

of reservoirs, it is observed that Rock Type 1 yields excellent reservoir capacity, which is consistent with Table 7, where lower rock type values indicate poorer reservoir quality (very poor). When examining the results of the three figures, the reservoir characterization of RT-4 results in the lowest quality, with the majority of the depth interval being classi-

fied as coal or dominated by shale. Hence, when analyzing the correlations of the MZG reservoirs, it has been determined that MZG-3 exhibits the highest reservoir capacity as per the designated marker. However, in terms of the prevalence of sand bodies relative to the oil-water interface, MZG-2 demonstrates superior performance.

3. Conclusion

The rock typing results obtained based on the hydraulic flow unit method amounted to 4 rock types. This determination is based on qualitative analysis, discrete rock type, scatter plot graph of mercury injection capillary pressure, and petrographic analysis (thin section). Rock type 1 (RT-1) is the best rock type category with the highest core porosity and core permeability values, while rock type 4 (RT-4) is the worst rock type category. The distribution of rock types using the Multi-Resolution Graph-Based Clustering method shows that the results obtained are well correlated based on the combination of rock typing processing parameters using the hydraulic flow unit method with petrophysical parameters, namely gamma ray, bulk density, neutron porosity, V_{shale}, and total porosity. Based on the original oil in place results, it was found that the MZG-3 tank obtained higher volume calculation results compared to the MZG1 and MZG-3 tanks. The effect of petrophysical calculations using parameter values a, m, and n based on SCAL and RCAL data with parameter values a, m, $n = 1, 2, 2$ produces an increase of 31% in tank 1 and 43% in tank 2 with values using a, m, and n based on SCAL and RCAL are higher in the results of oil reserve capacity (original oil in place) in this reservoir.

Acknowledgments. The authors would like to acknowledge the support received from Pertamina Hulu Indonesia Zone 9 for providing access to field data, which played a crucial role in supporting this study.

References

Abdulelah H., Mahmood S. and Hamada G. Hydraulic flow units for reservoir characterization: A successful application on arab-d carbonate // IOP Conference Series: Materials Science and Engineering. Vol. 380. — IOP Publishing, 2018. — P. 012020. — https://doi.org/10.1088/1757-899x/380/1/012020.

Adrianto R. D. PENENTUAN FLOW UNIT BATUAN RESERVOIR PADA LAPANGAN RN // PETRO:Jurnal Ilmiah Teknik Perminyakan. — 2018. — Vol. 6, no. 1. — P. 21–31. — https://doi.org/10.25105/petro.v6i1.2500.

Amaefule J. O., Altunbay M., Tiab D., et al. Enhanced Reservoir Description: Using Core and Log Data to Identify Hydraulic (Flow) Units and Predict Permeability in Uncored Intervals/Wells // SPE Annual Technical Conference and Exhibition. — Houston, Texas, 1993. — https://doi.org/10.2118/26436-ms.

Chambers J. L. C. and Daley T. E. A tectonic model for the onshore Kutai Basin, East Kalimantan // Geological Society, London, Special Publications. — 1997. — Vol. 126, no. 1. — P. 375–393. — https://doi.org/10.1144/gsl.sp.1997.126.01.23.

Cloke I. R., Moss S. J. and Craig J. Structural controls on the evolution of the Kutai Basin, East Kalimantan // Journal of Asian Earth Sciences. — 1999. — Vol. 17, no. 1/2. — P. 137–156. — https://doi.org/10.1016/s0743-9547(98)00036-1.

Corbett P. W. M. and Potter D. K. Petrotyping: A basemap and atlas for navigating through permeability and porosity data for reservoir comparison and permeability prediction // International Symposium of the Society of Core Analysts. Vol. 5. — 2004. — P. 1–12.

Ebanks W. J. Flow Unit Concept-Integrated Approach to Reservoir Description for Engineering Projects // AAPG Bulletin. — 1987. — Vol. 71. — P. 551–552. — https://doi.org/10.1306/94887168-1704-11D7-8645000102C1865D.

Guo G., Diaz M. A., Paz F., et al. Rock Typing as an Effective Tool for Permeability and Water-Saturation Modeling: A Case Study in a Clastic Reservoir in the Oriente Basin // SPE Reservoir Evaluation & Engineering. — 2007. — Vol. 10, no. 6. — P. 730–739. — https://doi.org/10.2118/97033-pa.

Hall R. and Nichols G. J. Cenozoic sedimentation and tectonics in Borneo: Climatic influences on orogenesis // Sediment Flux to Basins: Causes, Controls and Consequences / ed. by S. J. Jones and L. Frostick. — Geological Society of London Special Publication, 2002. — P. 5–22. — https://doi.org/10.1144/GSL.SP.2002.191.01.02.

McClay K., Dooley T. P., Ferguson A., et al. Tectonic evolution of the Sanga Sanga Block, Mahakam Delta, Kalimantan, Indonesia // AAPG Bulletin. — 2000. — Vol. 84, no. 6. — P. 765–786. — https://doi.org/10.1306/A96733EC-1738-11D7-8645000102C1865D.

Musu J. T., Permadi P. and Widarsono B. Connecting Microscopic Geological Features to Pore Geometry and Pore Structure: Case Study - Sandstone Reservoir of Balikpapan Formation, Kutai Basin // Modern Applied Science. — 2017. — Vol. 12, no. 1. — P. 51. — https://doi.org/10.5539/mas.v12n1p51.

Opuwari M., Amponsah-Dacosta M., Mohammed S., et al. Delineation of sandstone reservoirs of Pletmos Basin offshore South Africa into Flow Units using Core Data // South African Journal of Geology. — 2020. — Vol. 123, no. 4. — P. 479–492. — https://doi.org/10.25131/sajg.123.0032.

Satyana A. H. Post-collisional tectonic escapes in Indonesia: Fashioning the Cenozoic history // Proceedings PIT IAGI Riau 2006, The 35th IAGI Annual Convention and Exhibition. — Pekanbaru - Riau : IAGI, 2006.

El-Sawy M. Z., Abuhagaza A. A., Nabawy B., et al. Rock typing and hydraulic flow units as a successful tool for reservoir characterization of Bentiu-Abu Gabra sequence, Muglad basin, southwest Sudan // Journal of African Earth Sciences. — 2020. — Vol. 171. — P. 103961. — https://doi.org/10.1016/j.jafrearsci.2020.103961.

Ye S. J. and Rabiller P. A New Tool for Electro-Facies Analysis: Multi-Resolution Graph-Based Clustering // SPWLA 41st Annual Logging Symposium. — Society of Petrophysicists, Well-Log Analysts, 2000.